Syntheses, Structures, and Properties of $RbScFAsO_4$ and $CsScFAsO_4$: Scandium-Containing Analogues of Potassium Titanyl Phosphate ($KTiOPO_4$)†

William T. A. Harrison*,‡ and Mark L. F. Phillips§

Department of Chemistry, University of Aberdeen, Aberdeen AB24 3UE, U.K., and Gemfire Corporation, 2471 East Bayshore Road, Suite 600, Palo Alto, California 94303

Received May 27, 1999. Revised Manuscript Received October 6, 1999

The syntheses, single-crystal structures, and some properties of $RbScFAsO_4$, and $CsScFAsO_4$, the first scandium-containing analogues of potassium titanyl phosphate ($KTiOPO_4$), are reported. In both phases, the distinct cis and trans ScO_4F_2 octahedra are essentially regular and lack the distinctive short Ti=O bonds seen in $KTiOPO_4$. The powder second harmonic generation responses of these phases are much smaller that that of $KTiOPO_4$. Crystal data: $RbScFAsO_4$, $M_r = 288.34$, orthorhombic, space group $Pna2_1$ (no. 33), $a = 13.687(4)$ Å, $b = 6.804(2)$ Å, $c = 11.248(2)$ Å, $V = 1047.5(5)$ Å^3, $Z = 8$, $R = 3.15\%$, $R_w = 3.95\%$ [1807 reflections with $I > 2\sigma(I)$]; $CsScFAsO_4$, $M_r = 335.78$, orthorhombic, space group $Pna2_1$ (no. 33), $a = 13.900(2)$ Å, $b = 6.9413(8)$ Å, $c = 11.219(2)$ Å, $V = 1082.4(2)$ Å^3, $Z = 8$, $R = 3.65\%$, $R_w = 4.14\%$ [2205 reflections with $I > 3\sigma(I)$].

Introduction

Potassium titanyl phosphate ($KTiOPO_4$, or KTP) is of outstanding practical importance for its nonlinear optical properties, in particular second harmonic generation (SHG).[1−3] Its noncentrosymmetric crystal structure,[4] which contains 16 atoms (two $ABOXO_4$ formula units) in the asymmetric unit, is remarkably accommodating with respect to chemical composition. Different charge combinations are possible, as $A^IB^{IV}OX^VO_4$ and $A^IB^VOX^{IV}O_4$, and numerous solid solutions exist. Substitution of the inter-octahedral B−O−B oxygen atoms by OH^- and F^- is also possible, resulting in $A^IB^{III}(F,OH)X^VO_4$ phases. Single-crystal studies[5] have shown the following species (in amounts greater than doping quantities) to occupy the A (univalent cation), B (octahedral), and X (tetrahedral) sites in a manner consistent with the charge balancing criterion: A site, Li^+, Na^+, K^+, Rb^+, Cs^+, Ag^+, Tl^+, NH_4^+; B site, Ti^{IV}, V^{IV}, Sn^{IV}, Ge^{IV}, Sb^V, Ta^V, Nb^V, Ga^{III}, Fe^{III}, Cr^{III}, V^{III}; X site, P^V, As^V, Si^{IV}, Ge^{IV}.

In terms of solid state/materials chemistry, a key task is to relate small changes in crystal structure with the huge differences observed in the optical properties of these phases.[2] Most octahedral-site substitutions for titanium cause a very large attenuation of SHG response, typically by a factor of 100 or more,[2] although the $Pna2_1$ space group is unchanged for most systems at ambient conditions. The SHG efficacy of titanium-containing KTP-type phases has been rationalized in terms of the tendency of the TiO_6 group to distort (vide infra),[6,7] which in turn is related to the d^0 electron configuration of Ti^{IV}. It is therefore of interest to explore whether other d^0 cations may substitute into the KTP structure. Small quantities (∼1%) of the d^0-configuraton Sc^{3+} were doped into $KTiOPO_4$ by Hörlin and Bolt[8] during their investigation of the conductivity properties of KTP-type materials. It seemed plausible to us that complete replacement of titanium(IV) by scandium(III) could occur, provided charge balance was maintained by fluoride/hydroxide incorporation.

In this paper, we report the syntheses, single-crystal structures, and some properties of $RbScFAsO_4$ and $CsScFAsO_4$, the first scandium-containing analogues of $KTiOPO_4$. It appears that scandium is the largest cation (ionic radius = 0.745 Å)[9] to fully occupy the KTP octahedral cation site. These phases also represent the first occurrence together of F^- and $[AsO_4]^{3-}$ in a KTP-type phase. On a more general note, the application of hydrothermal synthesis in preparing oxofluoro anions of the type $[MOF_5]^{2-}$ and $[MO_2F_4]^{2-}$ has recently been described.[10]

Experimental Section

Synthesis of $RbScFAsO_4$. Initially, RbH_2AsO_4 was synthesized by heating As_2O_3 (Fisher) with 30% H_2O_2 (Fisher)

* Author for correspondence.
† Dedicated to the memory of Ted Gier 1924−1999.
‡ University of Aberdeen.
§ Gemfire Corporation.

(1) Zumsteg, F. C.; Bierlein, J. D.; Gier, T. E. *J. Appl. Phys.* **1976**, *47*, 4980.
(2) Stucky, G. D.; Phillips, M. L. F.; Gier, T. E. *Chem. Mater.* **1989**, *1*, 492 and references cited therein.
(3) Hagerman M. E.; Poeppelmeier, K. R. *Chem. Mater.* **1995**, *7*, 602 and references cited therein.
(4) Tordjman, I.; Masse, R.; Guitel, J. C. *Z. Kristallogr.* **1974**, *139*, 103.
(5) Data from the Inorganic Crystal Structure Database (ICSD), Version 98-01 (January 1998).
(6) Bergman J. G.; Crane, G. R. *J. Solid State Chem.* **1975**, *12*, 172.
(7) Burdett J. K.; Hughbanks, T. *Inorg. Chem.* **1985**, *24*, 1741.
(8) Hörlin T.; Bolt, R. *Solid State Ionics* **1995**, *78*, 55.
(9) Shannon, R. D. *Acta Crystallogr.* **1976**, *A32*, 751.
(10) Norquist, A. J.; Heier, K. R.; Stern, C. L.; Poeppelmeier, K. R. *Inorg. Chem.* **1998**, *37*, 6495.

10.1021/cm990335j CCC: $18.00
Published on Web 11/13/1999

until solution was complete. The resulting H_3AsO_4 was titrated with a 50% solution of RbOH (Aldrich), boiled until syrupy, drowned in methanol, filtered, and oven-dried at 100 °C. $RbScFAsO_4$ was prepared from 0.138 g (1 mmol) of Sc_2O_3 (Varlacoid Chemical Corp.), 2.264 g (10 mmol) of RbH_2AsO_4, 0.418 g (4 mmol) of RbF (Johnson Matthey), and 1.0 g of deionized water. These components were loaded into an Au tube (Engelhard; $^1/_4$ in. o.d. × 4 in. long × 0.007 in. wall thickness) that had been previously crimped and welded at one end. After the open end was sealed, the tube was placed in a steel bomb which was filled with water and placed in a Leco Tem-Pres HR-1B-2VH hydrothermal system. The bomb was cold pressurized to 1.9 kbar, heated to 700 °C, and periodically vented to yield a maximum pressure of 4.1 kbar. After soaking at 700 °C and 4.1 kbar for 12 h, the bomb was cooled to 500 °C at a rate of 2 °C/min and then to 350 °C at a rate of 6 °C/min and then cooled to room-temperature overnight. After removal from the bomb, the gold tube was expanded by gentle heating and then cut open, and the contents were recovered by filtration. The yield was 0.454 g of rhomboidal/irregular, clear, crystals and white powder of $RbScFAsO_4$.

Synthesis of $CsScFAsO_4$. Initially, CsH_2AsO_4 was prepared in the same way as RbH_2AsO_4, with CsOH replacing RbOH as a starting material. Then, 0.138 g (1 mmol) Sc_2O_3, 2.738 g (10 mmol) CsH_2AsO_4, 0.608 g (4 mmol) CsF and 1.0 g deionized water were loaded into a gold tube (dimensions as above) and welded shut. The sealed gold tube was subjected to the same temperature/pressure regime as for $RbScFAsO_4$, resulting in 1.34 g of irregular crystals and white powder of $CsScFAsO_4$.

Characterization. TGA/DTA for well-ground $RbScFAsO_4$ (ramp at 5 °C/min under air on a Rigaku Thermoflex instrument) showed no weight change over the range 25−900 °C. An endothermic event at ~576 °C was just discernible. TGA/DTA for $CsScFAsO_4$ resulted in a negligible weight loss between 25 and 900 °C and an endotherm at 663 °C. These DTA endotherms might accompany a strongly second-order ferroelectric → paraelectric phase transition which is known to occur at elevated temperatures for many KTP-type phases.[11−13]

Powder second harmonic generation (PSHG) data were recorded for well-ground samples of both title materials, using methods described previously.[14] $RbScFAsO_4$ showed a response of 0.5 that of quartz, and $CsScFAsO_4$, 1.2 that of quartz. These nonzero responses are strongly indicative of a noncentrosymmetric space group and are consistent with the successful refinements described below.

Powder X-ray data for a well-ground, white powder sample of $RbScFAsO_4$ were collected on a Siemens D5000 automated powder diffractometer [Cu Kα radiation, $\lambda = 1.541\,78$ Å, $T = 25(2)$ °C]. The application of software $K\alpha_2$ stripping and peak-fitting routine established peak positions relative to the Cu $K\alpha_1$ wavelength ($\lambda = 1.540\,56$ Å). There were many overlapped peaks, and *hkl* indices were cautiously assigned on the basis of comparison with a LAZY−PULVERIX[15] simulation of the single-crystal structure of $RbScFAsO_4$. Least-squares minimization using the program UNITCELL[16] led to refined lattice parameters of $a = 13.663(3)$ Å, $b = 6.788(2)$ Å, and $c = 11.220(2)$ Å [$V = 1040.6(3)$ Å^3] for $RbScFAsO_4$ as listed in Table 1. The application of similar data collection and analysis procedures for $CsScFAsO_4$ resulted in refined lattice constants of $a = 13.874(2)$ Å, $b = 6.930(2)$ Å, and $c = 11.195(3)$ Å [$V = 1076.4(3)$ Å^3], as listed in Table 2. These was no evidence for impurity phases in either sample, except for possibly trace quantities of Sc_2O_3.

Table 1. Powder X-ray Data for $RbScFAsO_4$

h	*k*	*l*	d_{obs} (Å)	d_{calc} (Å)	Δd (Å)	I_{rel}
2	0	1	5.830	5.836	−0.006	14
2	0	2	4.330	4.335	−0.005	44
3	1	0	3.784	3.782	0.002	25
2	1	2	3.650	3.654	−0.003	75
3	1	1	3.586	3.584	0.003	28
4	0	0	3.416	3.416	0.000	19
0	1	3	3.276	3.276	0.001	100
1	2	1	3.161	3.161	0.001	19
4	1	1	2.945	2.944	0.000	56
0	0	4	2.805	2.805	0.001	13
2	2	2	2.671	2.673	-0.002	3
3	2	2	2.447	2.449	−0.002	9
4	2	0	2.409	2.408	0.001	10
2	2	3	2.360	2.359	0.001	25
5	1	2	2.311	2.310	0.001	22
1	3	0	2.232	2.232	0.000	28
0	1	5	2.131	2.131	0.000	9
1	3	2	2.073	2.074	−0.001	6
6	1	2	2.014	2.015	−0.001	18
6	0	3	1.9449	1.9450	0.0000	15
3	3	2	1.9066	1.9059	0.0007	29
7	1	1	1.8507	1.8502	0.0005	19
4	2	4	1.8268	1.8269	−0.0002	33
4	1	5	1.8077	1.8077	0.0000	18
7	1	3	1.6760	1.6768	−0.0008	15
2	0	7	1.5606	1.5604	0.0002	12

Table 2. Powder X-ray Data for $CsScFAsO_4$

h	*k*	*l*	d_{obs} (Å)	d_{calc} (Å)	Δd (Å)	I_{rel}
0	1	1	5.887	5.893	−0.006	6
3	1	0	3.848	3.847	0.001	19
2	1	2	3.692	3.688	0.004	27
3	1	1	3.638	3.638	0.000	10
4	0	0	3.468	3.468	−0.001	49
4	0	1	3.313	3.313	0.000	20
0	1	3	3.283	3.286	−0.002	33
1	2	1	3.216	3.220	−0.004	8
2	2	0	3.102	3.100	0.002	3
4	1	1	2.988	2.989	-0.001	100
0	2	2	2.945	2.946	−0.001	26
1	2	2	2.882	2.882	0.000	6
0	0	4	2.800	2.799	0.001	5
5	1	0	2.578	2.576	0.002	4
4	2	0	2.452	2.451	0.000	10
4	1	3	2.384	2.385	−0.001	6
5	1	2	2.341	2.340	0.001	8
6	0	0	2.313	2.312	0.000	21
6	0	1	2.264	2.264	−0.001	14
3	2	3	2.227	2.226	0.002	4
4	0	4	2.177	2.178	−0.001	7
6	1	1	2.152	2.152	−0.001	3
0	1	5	2.131	2.131	0.001	8
6	1	2	2.043	2.042	0.000	18
0	3	3	1.9645	1.9641	0.0004	8
6	2	0	1.9236	1.9234	0.0002	5
4	3	1	1.8946	1.8949	−0.0003	8
7	1	1	1.8785	1.8786	−0.0001	12
4	2	4	1.8431	1.8440	−0.0010	11
8	0	0	1.7338	1.7342	−0.0005	10
8	2	0	1.5512	1.5508	0.0004	9

Structure Determinations. A crystal of $RbScFAsO_4$ (transparent, rounded block ~0.2 × 0.3 × 0.3 mm) was glued to a thin glass fiber with cyanoacrylate adhesive and mounted on a Siemens P4 automated diffractometer (graphite-monochromated Mo Kα radiation, $\lambda = 0.710\,73$ Å). A primitive orthorhombic unit cell (Table 3) was established and optimized by the application of peak-search, centring, indexing and least-squares routines (30 reflections, $14° < 2\theta < 20°$).

Two octants of intensity data [(−,−,−) and (+,+,+)] were collected at room temperature using the $\theta/2\theta$ scan mode to a maximum 2θ of 55°. Intensity standards, remeasured every

(11) Harrison, W. T. A.; Gier, T. E.; Stucky, G. D.; Schultz, A. J. *J. Chem. Soc., Chem. Commun.* **1990**, 540.
(12) Northrup, P. A.; Parise, J. B.; Cheng, L. K.; Cheng, L. T.; McCarron, E. M. *Chem. Mater.* **1994**, *6*, 434.
(13) Favard, J.-F.; Verbaere, A.; Piffard, Y.; Tournoux, M. *Eur J. Solid State Inorg. Chem.* **1994**, *31*, 995.
(14) Dougherty J. P.; Kurtz, S. K. *J. Appl. Crystallogr.* **1976**, *9*, 145.
(15) Yvon, K.; Jeitschko, W.; Parthe, E. *J. Appl. Crystallogr.* **1977**, *10*, 73.
(16) Holland, T. J. B.; Redfern, S. A. T. *Mineral. Mag.* **1997**, *61*, 65.

Table 3. Crystallographic Parameters

	$RbScFAsO_4$	$CsScFAsO_4$
empirical formula	$RbAsScFO_4$	$CsAsScFO_4$
fw	288.34	335.78
cryst syst	orthorhombic	orthorhombic
a (Å)	13.687(4)	13.900(2)
b (Å)	6.804(2)	6.9413(8)
c (Å)	11.248(2)	11.219(2)
V (Å^3)	1047.5(5)	1082.4(2)
Z	8	8
space group	$Pna2_1$ (no. 33)	$Pna2_1$ (no. 33)
T (°C)	25(2)	25(2)
λ(Mo Kα) (Å)	0.710 73	0.710 73
ρ_{calc} (g/cm^3)	3.66	4.12
μ (cm^{-1})	168.5	139.5
total no. of data	3446	3806
no. of obsd data	1807[a]	2205[b]
no. of params	147	157
min, max $\Delta\rho$ (e/Å^3)	−1.47, +2.00	−2.03, +2.85
$R(F)$[c]	3.15	3.65
$R_w(F)$[d]	3.95	4.14

[a] $I > 2\sigma(I)$ after data merging. [b] $I > 3\sigma(I)$ after data merging. [c] $R = 100 \times \sum||F_o| - |F_c||/\sum|F_o|$. [d] $R_w = 100 \times [\sum(|F_o| - |F_c|)^2/\sum w|F_o|^2]^{1/2}$ with w_i as described in the text.

100 observations, showed only statistical fluctuations over the course of the data collection. Absorption was monitored by ψ scans, and a correction (equivalent transmission factor range: 0.060−0.098) was applied at the data reduction stage. The 3446 raw intensities were reduced to F and $\sigma(F)$ values, the normal corrections for Lorentz and polarization effects were made, and the equivalent data were merged to yield 2319 unique reflections [1807 considered observed according to the criterion $I > 2\sigma(I)$] with $R_{int} = 0.033$.

The systematic absences in the reduced data indicated space groups $Pna2_1$ (no. 33), as observed for most other KTP-type phases,[2] or *Pnam* (no. 62). Centrosymmetric *Pnam* is not consistent with a nonzero PSHG response, and no other KTP-type phases have been reported to crystallize in this symmetry. Attempts to model the $RbScFAsO_4$ structure in *Pnam* were not successful. The crystal structure model for $RbScFAsO_4$ was developed in space group $Pna2_1$ (no. 33) using the atomic coordinates of $KVOPO_4$[17] [Rb substituting for K; Sc for V; As for P] as a starting model for the heavy atoms. This distribution of Rb^I, Sc^{III}, and As^V requires nine negative charges per formula unit for charge balance, i.e., four O^{2-} and one OH^- or F^-. Initial refinements [$R_w = 4.3\%$] with all 10 anion sites given pure O atom character led to nonpositive definite thermal factors for the inter-scandium bridging species, O9 and O10. These two sites were then assigned a mixture of O and F character. Refinements subject to the constraints occ[O9] + occ[F9] = 1.00 and occ[O10] + occ[F10] = 1.00 led to pure F atom character for both sites within experimental error (typical site occupation esd ≈ 0.1), physically reasonable thermal parameters, and lower residuals. The final cycles of refinement simply modeled these species as F atoms. Final residuals of $R = 3.15\%$ and $R_w = 3.95\%$ (w_i described by a three-term Chebychev polynomial[18]) were obtained for refinements varying positional and anisotropic thermal parameters for all atoms, a Larson-type secondary extinction correction,[19] and the Flack absolute structure parameter.[20] The Flack parameter refined to 0.15(2), perhaps indicating a degree of merohedral twinning in the crystal examined here. There were small difference Fourier peaks ($\Delta\rho_{max} < 2$ e Å^{-3}) near both the Rb atoms. Refinements based on a disordered model for these species were unstable, with high correlations, and did not converge (vide infra). All the crystallographic calculations were performed with the Oxford CRYSTALS[21] system, using complex neutral-atom scattering factors.[22] Crystallographic data are summarized in Table 3. Because of the pseudo-symmetry present (vide infra) an additional refinement was performed in the centrosymmetric space group *Pnan* (no. 52).[11] This converged with significantly poorer residuals ($R \approx 10\%$) than the $Pna2_1$ model.

Table 4. Atomic Coordinates/Thermal Factors for $RbScFAsO_4$

atom	x	y	z	U_{eq}[a]	BVS[b]
Rb1	0.37979(8)	0.7753(2)	0.2894(2)	0.0284	1.02
Rb2	0.10573(7)	0.6982(2)	0.0459(2)	0.0283	0.91
Sc1	0.38716(9)	0.4959(3)	-0.0183(2)	0.0095	3.08
Sc2	0.2461(2)	0.2519(3)	0.2307(2)	0.0093	3.01
As1	0.49866(7)	0.3239(2)	0.2326(2)	0.0094	5.12
As2	0.18241(5)	0.4990(2)	0.4838(2)	0.0098	4.99
O1	0.4841(6)	0.483(2)	0.1194(8)	0.0173	2.15
O2	0.5103(6)	0.465(2)	0.3535(7)	0.0161	2.18
O3	0.3974(4)	0.187(1)	0.2512(7)	0.0165	1.99
O4	0.5975(5)	0.184(2)	0.2129(6)	0.0137	1.91
O5	0.1122(5)	0.302(1)	0.5149(6)	0.0168	1.97
O6	0.1136(5)	0.696(1)	0.4586(7)	0.0195	1.89
O7	0.2572(6)	0.536(2)	0.6036(7)	0.0160	1.93
O8	0.2569(6)	0.453(2)	0.3686(7)	0.0177	2.06
F9	0.2741(5)	0.468(1)	0.1099(6)	0.0161	1.02
F10	0.2244(5)	0.039(1)	0.3605(5)	0.0150	1.01

[a] U_{eq} (Å^2) = $^1/_3[U_1 + U_2 + U_3]$. [b] Bond valence sums (expected values: Rb 1.00, Sc 3.00, As 5.00, O 2.00, F 1.00).

The structure determination (Table 3) for $CsScFAsO_4$ followed a similar procedure to that for the rubidium phase: transparent, rounded block ∼0.2 × 0.3 × 0.3 mm; room temperature; primitive orthorhombic unit cell from 24 reflections, 20° < 2θ < 25°; (−,−,−) and (+,+,+) octants collected; $2\theta_{max} = 60°$; absorption correction (0.049−0.146) from ψ scans; 3809 data, 2500 merged data [2205 with $I > 3\sigma(I)$] with $R_{int} = 0.041$; initial crystal structure model in space group $Pna2_1$ from that of $RbScFAsO_4$ (Cs replacing Rb). Attempts at refining the structure in *Pnam* failed. After all the atoms had been refined anisotropically [$R(F) = 4.06\%$], difference Fourier maps for $CsScFAsO_4$ were noisier that expected ($\Delta\rho_{max} \approx 5$ e Å^{-3}) in the vicinity of the cesium cations. A model involving partial disorder of both the Cs^+ species was developed, with occupancy constraints [occ(Cs1) + occ(Cs11) = 1.00 and occ(Cs2) + occ(Cs12) = 1.00] applied to stabilize the refinement. In this case, convergence was achieved, and improved final residuals of $R = 3.65\%$ and $R_w = 4.14\%$ were obtained for refinements varying positional and anisotropic thermal parameters for all atoms (U_{iso} for Cs11 and Cs12). The refined value of the Flack parameter, 0.48(2), indicated a merohedrally twinned (random 50:50 mixture of both enantiomers) sample.

Results

Crystal Structure of $RbScFAsO_4$. Atomic positional and thermal factors for $RbScFAsO_4$ are listed in Table 4, with selected geometrical data in Table 5. The building unit of this phase is illustrated in Figure 1, with the complete crystal structure displayed in Figure 2. $RbScFAsO_4$ is another isostructure of the $KTiOPO_4$ family,[2] built up from Rb^+ cations, ScO_4F_2 octahedra, and AsO_4 tetrahedra. Sc−F−Sc and Sc−O−As bonds provide the inter-polyhedral links.

The two distinct rubidium cations in $RbScFAsO_4$ show irregular coordination: Rb1 is eight-coordinate to six O and two F atoms [$d_{av} = 3.034(7)$ Å] and Rb2 is nine-coordinate to seven O and two F [$d_{av} = 3.121(7)$ Å]. The

(17) Phillips, M. L. F.; Harrison, W. T. A.; Gier, T. E.; Stucky, G. D.; Kulkarni, G. V.; Burdett, J. K. *Inorg. Chem.* **1990**, *29*, 2158.
(18) Carruthers, J. R.; Watkin, D. J. *Acta Crystallogr.* **1979**, *A35*, 698.
(19) Larson, A. C. *Acta Crystallogr.* **1967**, *23*, 664.
(20) Flack, H. D. *Acta Crystallogr.* **1983**, *A39*, 876.
(21) Watkin, D. J.; Carruthers, J. R.; Betteridge, P. W. *CRYSTALS User Guide*; Chemical Crystallography Laboratory, University of Oxford: Oxford, U.K., 1999.
(22) *International Tables for Crystallography*; Kynoch Press: Birmingham, U.K., 1974; Vol. IV.

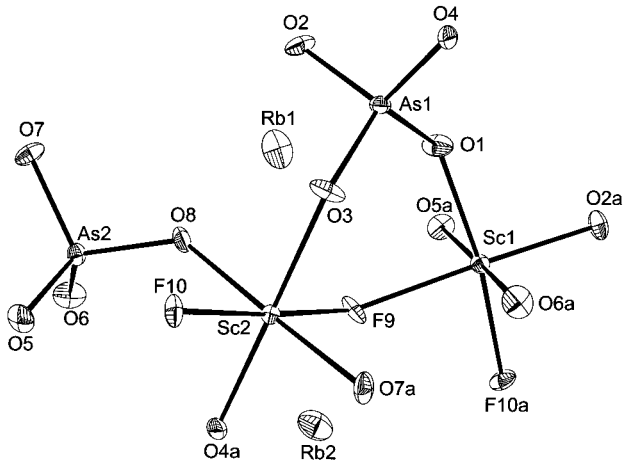

Figure 1. Fragment of the $RbScFAsO_4$ structure showing the octahedral/tetrahedral building units (50% thermal ellipsoids). Symmetry related atoms are denoted as, e.g., O2a.

Table 5. Selected Bond Distances (Å) and Angles (deg) for $RbScFAsO_4$

Rb1−O1	3.108(9)	Rb1−O2	2.861(9)
Rb1−O3	2.843(7)	Rb1−O5	3.095(7)
Rb1−O7	3.321(9)	Rb1−O8	2.902(8)
Rb1−F9	3.247(7)	Rb1−F10	2.893(7)
Rb2−O1	2.857(8)	Rb2−O2	3.239(9)
Rb2−O3	3.316(8)	Rb2−O4	3.211(7)
Rb2−O5	3.003(7)	Rb2−O7	3.036(8)
Rb2−O8	3.24(1)	Rb2−F9	2.878(7)
Rb2−F10	3.307(7)		
Sc1−O1	2.041(8)	Sc1−O2	2.030(8)
Sc1−O5	2.113(7)	Sc1−O6	2.055(7)
Sc1−F9	2.124(6)	Sc1−F10	2.068(7)
Sc2−O3	2.131(6)	Sc2−O4	2.089(7)
Sc2−O7	2.050(8)	Sc2−O8	2.075(9)
Sc2−F9	2.038(7)	Sc2−F10	2.080(7)
As1−O1	1.683(8)	As1−O2	1.670(8)
As1−O3	1.683(6)	As1−O4	1.668(7)
As2−O5	1.688(7)	As2−O6	1.664(7)
As2−O7	1.711(8)	As2−O8	1.678(8)
Sc1−O1−As1	132.8(5)	Sc1−O2−As1	136.1(5)
Sc2−O3−As1	132.2(4)	Sc2−O4−As1	131.2(4)
Sc1−O5−As2	138.1(4)	Sc1−O6−As2	141.4(4)
Sc2−O7−As2	129.9(4)	Sc2−O8−As2	131.0(4)
Sc1−F9−Sc2	130.8(3)	Sc1−F10−Sc2	131.8(4)

ScO_4F_2 octahedra are fairly regular, with d_{av}(Sc1−O,F) = 2.072(6) Å and d_{av}[Sc2−O,F] = 2.077(6) Å. Octahedral displacements of Δ_{oct} = 0.06 Å for Sc1 and Δ_{oct} = 0.03 Å for Sc2, where Δ_{oct} is the displacement of the Sc species from the geometric centroid[23] of its octahedron, arise. These octahedral displacements are much smaller than those ($\Delta_{oct} \geq \sim$0.20 Å) seen in Ti^{IV} and V^{IV}-containing KTP isostructures,[2,3] and there are no unusually short Sc−F bonds akin to the formal Ti=O and V=O double bonds seen in $RbTiOAsO_4$[24] or $KVOPO_4$,[17] respectively. The AsO_4 tetrahedra are typical [d_{av}(As1−O) = 1.676(6) Å, d_{av}(As2−O) = 1.685(6) Å] and compare well to the equivalent groupings [d_{av}(As−O) = 1.685 Å] seen in $RbTiOAsO_4$. The average Sc−O−As bond angle is 133.5°, compared to the average Ti−O−As bond angle of 130.2° in $RbTiOAsO_4$. Bond valence sum (BVS) values calculated by the Brown formalism,[25] as listed in Table 4, are in good accordance with the expected values (Rb, 1.00; Sc, 3.00; As, 5.00; O, 2.00; F, 1.00). The average bond valence sum of the eight O atoms is 2.01.

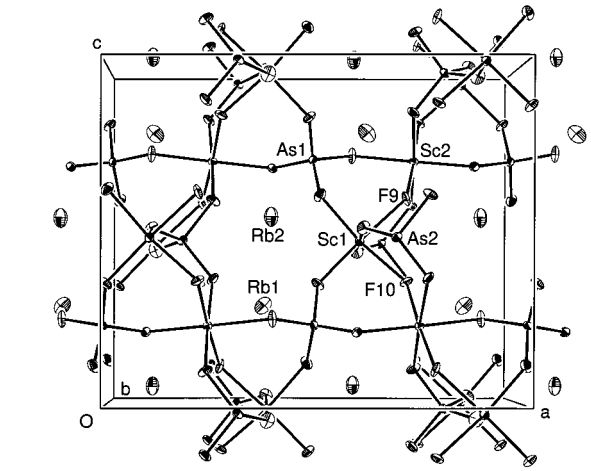

Figure 2. View down [010] of the unit cell packing in $RbScFAsO_4$ with selected atom labeled.

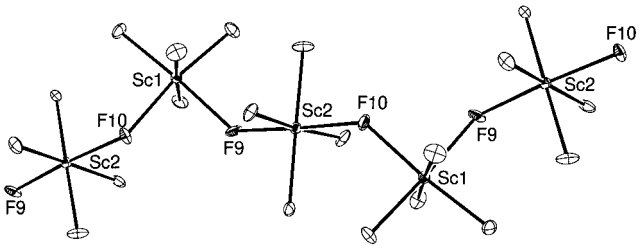

Figure 3. Fragment of an infinite chain of ScO_4F_2 octahedra in $RbScFAsO_4$. Note the Sc−F−Sc links, the cis configuration of the F atoms around Sc1, and the trans configuration of F about Sc2.

The polyhedral connectivity in $RbScFAsO_4$ results in a three-dimensional network of vertex-sharing octahedra and tetrahedra.[2] The ScO_4F_2 octahedra form infinite chains which propagate along [011] and [0$\bar{1}$1] in zigzag fashion,[2,3] with the fluoride ions providing the Sc−F−Sc links. Alternate octahedra are cis and trans linked with respect to the chains (Figure 3). Arsenic atoms cross-link the octahedral chains (as $[AsO_4]^{3-}$ arsenate tetrahedra). The resulting network contains corrugated channels aligned along [001], the polar axis direction. The rubidium cations occupy these channels in similar sites to those of the corresponding species in $RbTiOAsO_4$ and most other KTP types. The Rb···Rb separations in the [001] channels [4.080(2) and 4.135(2) Å] are somewhat larger than those seen in $RbTiOAsO_4$ [3.825(5) and 4.055(5) Å].

Crystal Structure of $CsScFAsO_4$. This phase also crystallizes as a $KTiOPO_4$ isostructure. Atomic positional and thermal factors are listed in Table 6, with selected geometrical data in Table 7. The unit cell is illustrated in polyhedral form in Figure 4.

The main feature of this phase is the partial disorder of the cesium species. Both Cs1 and its partner Cs11, and Cs2 + Cs12 are barely resolvable from the present data [d(Cs1···Cs11) = 0.60(2) Å; d(Cs1···Cs12) = 0.57(3) Å]. Cs1 dominates Cs11 in a ~92:8 ratio, with a similar situation for Cs2/Cs12 (~94:6). The displacement of the

(23) Zunic, T. B.; Makovicky, E. *Acta Crystallogr.* **1996**, *B52*, 78.
(24) Thomas, P. A.; Mayo, S. C. Watts, B. E. *Acta Crystallogr.* **1992**, *B48*, 401.
(25) Brown, I. D. *J. Appl. Crystallogr.* **1996**, *29*, 479.

Table 6. Atomic Coordinates/Thermal Factors for CsScFAsO$_4$

atom	*x*	*y*	*z*	U_{eq}[a]	BVS[b]	occ[c]
Cs1	0.38647(5)	0.78128(8)	0.3124(4)	0.0262	1.19	0.916(8)
Cs2	0.10711(4)	0.6972(1)	0.0592(3)	0.0225	1.14	0.942(9)
Cs11	0.8913(5)	0.709(2)	0.365(2)	0.023(3)	1.01	0.084(8)
Cs12	0.1096(8)	0.709(2)	0.109(3)	0.021(4)	1.14	0.058(9)
Sc1	0.38609(7)	0.4971(2)	−0.0160(5)	0.0086	3.01	
Sc2	0.24636(9)	0.2525(2)	0.2325(5)	0.0089	2.93	
As1	0.49922(5)	0.32286(8)	0.2333(5)	0.0085	5.04	
As2	0.17971(4)	0.5010(1)	0.4852(5)	0.0093	4.93	
O1	0.4842(4)	0.4781(9)	0.1187(7)	0.0174	2.18	
O2	0.5148(4)	0.4593(9)	0.3552(7)	0.0153	2.25	
O3	0.3975(3)	0.1957(7)	0.2547(8)	0.0138	2.00	
O4	0.5968(4)	0.1863(7)	0.2098(7)	0.0134	1.88	
O5	0.1144(4)	0.3019(8)	0.5184(8)	0.0157	1.90	
O6	0.1121(4)	0.6973(7)	0.4569(9)	0.0162	1.80	
O7	0.2538(4)	0.5458(9)	0.6010(7)	0.0161	2.00	
O8	0.2523(4)	0.4536(9)	0.3677(7)	0.0182	2.06	
F9	0.2772(3)	0.4618(7)	0.1100(6)	0.0151	1.09	
F10	0.2229(3)	0.0436(7)	0.3604(6)	0.0171	1.07	

[a] U_{eq} (Å^2) = $^1/_3[U_1 + U_2 + U_3]$. [b] Bond valence sums (expected values: Cs 1.00, Sc 3.00, As 5.00, O 2.00, F 1.00). [c] Fractional site occupancy, if not unity.

Table 7. Selected Bond Distances (Å) and Angles (deg) for CsScFAsO$_4$

Cs1−O1	3.316(7)	Cs1−O2	2.899(6)
Cs1−O3	2.953(5)	Cs1−O5	3.301(8)
Cs1−O6	3.534(6)	Cs1−O7	3.578(7)
Cs1−O8	3.006(6)	Cs1−F9	3.519(5)
Cs1−F10	2.962(5)		
Cs2−O1	2.906(6)	Cs2−O2	3.379(7)
Cs2−O3	3.417(8)	Cs2−O4	3.156(6)
Cs2−O5	3.113(5)	Cs2−O7	3.132(6)
Cs2−O8	3.407(7)	Cs2−F9	2.930(5)
Cs2−F10	3.420(5)		
Sc1−O1	2.040(6)	Sc1−O2	2.020(6)
Sc1−O5	2.151(5)	Sc1−O6	2.103(5)
Sc1−F9	2.086(5)	Sc1−F10	2.080(5)
Sc2−O3	2.153(5)	Sc2−O4	2.138(5)
Sc2−O7	2.058(6)	Sc2−O8	2.063(6)
Sc2−F9	2.045(5)	Sc2−F10	2.066(5)
As1−O1	1.690(6)	As1−O2	1.677(6)
As1−O3	1.683(5)	As1−O4	1.675(5)
As2−O5	1.695(5)	As2−O6	1.686(5)
As2−O7	1.686(6)	As2−O8	1.693(6)
Sc1−O1−As1	133.4(3)	Sc1−O2−As1	139.1(4)
Sc2−O3−As1	135.0(3)	Sc2−O4−As1	131.0(3)
Sc1−O5−As2	139.9(3)	Sc1−O6−As2	140.0(3)
Sc2−O7−As2	132.8(3)	Sc2−O8−As2	132.9(3)
Sc1−F9−Sc2	133.7(2)	Sc1−F10−Sc2	133.4(2)

minor partner from the major partner is essentially along [001], the polar axis, in both cases. Whether this situation represents well-defined cation disorder over two sites, as previously seen in $Na_{0.58}K_{0.42}TiOPO_4$,[26] or is a "ghosting" artifact of the refinement in a polar space group[27,28] is not totally clear. As modeled here, both Cs1 and Cs2 are nine coordinate to seven O and two F atoms [d_{av}(Cs1−O,F) = 3.230(5) Å, d_{av}(Cs2−O,F) = 3.207(5) Å], assuming a maximum Cs-to-anion contact distance of 3.6 Å. Within this distance limit, Cs11 and Cs12 are only five-coordinate to O or F, but when very long (up to 3.8 Å) Cs···O,F distances are considered, their coordination numbers rise to 8-fold and 7-fold, respectively. The BVS values listed in Table 6 are reasonable, albeit with a suggestion that the majority site cesium cations are slightly "overbonded," compared to their expected BVS values of 1.00. The average bond valence of the oxygen atoms is 2.01.

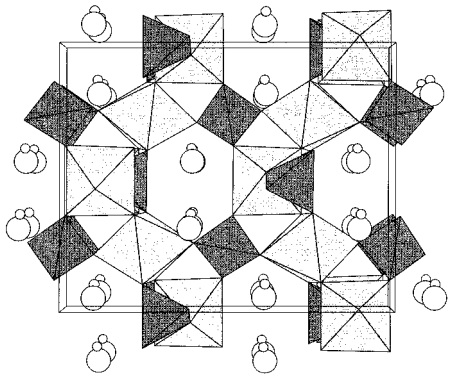

Figure 4. Polyhedral view down [010] of the CsScFAsO$_4$ structure, showing the vertex-sharing ScO_4F_2 octahedral (light shading) + AsO_4 tetrahedral (darker shading) framework. Cs species are represented by large circles (Cs1 and Cs2) and small circles (Cs11 and Cs12).

The ScO_4F_2 octahedra are essentially regular, with d_{av}(Sc1−O,F) = 2.080(4) Å and d_{av}[Sc2−O,F] = 2.087(4) Å. Octahedral displacements of Δ_{oct}(Sc1) = 0.04 Å and Δ_{oct}(Sc2) = 0.01 Å arise, and as with RbScFAsO$_4$, we cannot identify any short Sc−F bonds akin to formal Ti═O titanyl links. The AsO_4 tetrahedra in CsScFAsO$_4$ are typical [d_{av}(As1−O) = 1.681(4) Å, d_{av}(As2−O) = 1.690(4) Å], and the average Sc−O−As bond angle is 135.5°.

Discussion

The new KTP-type phases RbScFAsO$_4$ and CsScFAsO$_4$ have been prepared by high-pressure hydrothermal methods and characterized by single-crystal X-ray diffraction methods and other techniques. They are the first $KTiOPO_4$-type phases to contain only scandium on the octahedral sites, further expanding the substitution chemistry for this versatile crystal structure. These phases are also the first KTP isostructures to feature the combination of inter-octahedral bridging fluoride ions and arsenate ions. The unit cell volume of CsScFAsO$_4$, 1082.4 Å^3, appears to be the largest reported for this structure type, and is some 24% greater than that of $KTiOPO_4$ ($V \approx 871$ Å^3).

At room temperature, RbScFAsO$_4$ and CsScFAsO$_4$ crystallize in the typical $Pna2_1$ space group for this family of structures,[2,29] but they differ significantly from titanium-containing KTP-types in the negligible distortion (i.e. displacement of the Sc cation from the octahedral center) of the ScO_4F_2 moieties and consequent lack of any short Sc−F links with multiple bond character, akin to the short Ti═O bonds in $KTiOPO_4$.[2] This is in accord with a symmetry analysis[30] which indicated that the $[ScFAsO_4]^-$ frameworks of both RbScFAsO$_4$ and CsScFAsO$_4$ have essentially *Pnan*

(26) Crenell, S. J.; Morris, R. E.; Cheetham, A. K.; Jarman, R. H. *Chem. Mater.* **1992**, *4*, 82.
(27) Womersley, M. N.; Thomas, P. A.; Corker, D. L. *Acta Crystallogr.* **1998**, *B54*, 635.
(28) Thomas P. A.; Womersley, M. N. *Acta Crystallogr.* **1998**, *B54*, 645.
(29) Schindler, M.; Joswig, W.; Baur, W. H. *J. Solid State Chem.* **1997**, *134*, 286.
(30) Farrugia, L. J. PLATON98 for Windows: www.chem.gla.ac.uk/~louis/software.

symmetry (the space group of the high temperature, paraelectric modification[11] of the KTP-type structure). However, the positions of the rubidium and cesium (majority site) cations are definitely not consistent with the higher symmetry. A similar *Pnan* pseudosymmetry effect for the $[SbOSiO_4]^-$ framework has been seen for the $MSbOSiO_4$ series.[13]

On the basis of the single-crystal refinement, $CsScFAsO_4$ is complicated by partial disorder of the cesium ions in the [001] channels. A similar effect may also apply for $RbScFAsO_4$, but it could not be reliably resolved from the present data. It is notable that a similar cation disorder effect has recently been observed at the cesium-rich end of $Cs_{1-x}Rb_xTiOAsO_4$ series.[27] Thomas et al. have discussed this phenomenon in detail[28] in terms of microtwinning and possible refinement artifacts arising from a pseudosymmetic structure in a polar space group. However, it appears that the correct space group for modeling these phases is $Pna2_1$.[28]

The inter-octahedral-site [O/F9 and O/F10 in our notation] fluorine substitution pattern proposed for $RbScFAsO_4$ and $CsScFAsO_4$ is supported by various evidence as well as the optimal refinements noted above. A precedent is set by phosphate KTP-type phases such as $KFeFPO_4$[31] and $KCrFPO_4$,[32] where the fluoride ions occupy only inter-octahedral sites. Bond valence sum calculations support the location of fluoride ions in the scandium fluoroarsenates as modeled here. For $RbScFAsO_4$, BVS values of 1.02 for F9 and 1.01 for F10 result, in excellent accordance with the expected value of 1.00 for F^-, when considering Sc−F and Rb−F interactions. Assuming oxide ions to occupy the same sites, then BVS values of 1.33 and 1.32, respectively, are obtained, substantially below the expected value of 2.00 for O^{2-}. A similar conclusion is reached for $CsScFAsO_4$ (Table 6). The TGA data indicate no weight loss to 900 °C, which is consistent with the proposed composition. An alternative situation involving bridging OH groups, as seen in $KGaF_{1-\delta}(OH)_\delta PO_4$ ($\delta \approx 0.3$),[33] would result in a measurable weight decrease due to loss of hydroxide as water.

The observation of very low PSHG responses for the title compounds is consistent with the empirical fact that distorted octahedral TiO_6 groups are required for a substantial (up to ∼1000× that of quartz) PSHG response to be seen in KTP-type phases.[2,3] In simple terms, titanium(IV) has a propensity to move away from the centroid of its octahedron, approximately along a Ti−O bond axis. This results in short, "titanyl" Ti═O bonds with a high degree of microscopic polarizability[6] and consequent substantial bulk optical response, according to symmetry constraints.[3] More detailed extended Hückel theory analyses TiO_6 octahedral distortions in terms of an extended band structure to arrive at a similar result.[7] It should be noted that the presence of short Ti═O bonds (for example, in $NaTiOAsO_4$) is not the *sole* criterion for a large SHG response in KTP-type phases: detailed structure−property studies[34] have shown that the univalent and tetrahedral (phosphorus or arsenic) cations play important roles in defining the overall SHG signal. However, all non-titanium-containing KTP-type phases reported so far, such as the $MSnOXO_4$ and $MGeOXO_4$ families, show essentially regular $Sn^{IV}O_6$ and $Ge^{IV}O_6$ octahedra and negligible SHG responses compared to $KTiOPO_4$, regardless of the identity of M or X.[2] Thus, the presence of undistorted ScO_4F_2 groups (and no short Sc−F bonds) in the $MScFAsO_4$ phases described here is not inconsistent with this simple phenomenological approach.

The broader question of *why* the $Ti^{IV}O_6$ group distort, and why other cations do not distort in $MTiOXO_4$ phases can be appreciated from a materials chemists' perspective[35] in terms of a second-order Jahn−Teller (SOJT) effect,[36] which requires a small energy difference between the highest occupied (HOMO) and lowest unoccupied (LUMO) molecular orbitals. In titanium-containing KTP types, the HOMO has largely oxygen 2p character, the LUMO has metal 3d character. The energy-lowering accompanying the SOJT effect is accompanied by a change in "structural energy" which is expected to militate *against* an octahedral distortion in most cases.[35] In KTP $Ti^{IV}O_6$ groups, the d−p HOMO−LUMO energy gap is small, and the SOJT effect is consequently significant, leading to a large octahedral distortion at ambient temperatures. In $Sc^{III}O_6$ groups, the d−p energy gap is substantially larger, and scandium rarely if ever shows a displacement-type octahedral distortion.[35] More detailed work would be necessary to precisely quantify the effect of fluoride ions in the scandium coordination sphere (i.e., the difference, if any, between ScO_6 groups, and the cis and trans $Sc^{III}O_4F_2$ groups found in the title compounds), but intuitively it seems likely that the d−p gap will be larger still and regular octahedra are thus expected.

Acknowledgment. We thank Vojislav Srdanov (University of California at Santa Barbara) for assistance with the PSHG measurements.

Supporting Information Available: Tables of anisotropic thermal factors and observed and calculated structure factors for both title phases. This material is available free of charge via the Internet at http://pubs.acs.org.

CM990335J

(31) Matvienko, E. N.; Yakubovich, O. V.; Simonov, M. A.; Belov, N. V. *Dokl. Akad. Nauk SSSR* **1979**, *246*, 875.
(32) Slobodyanik, N. S.; Nagornyi, P. G.; Kornienko, Z. I.; Kapshuk, A. A. *Zh. Neorg. Khim.* **1991**, *36*, 1390.
(33) Harrison, W. T. A.; Phillips, M. L. F.; Stucky, G. D. *Chem. Mater.* **1995**, *7*, 1849.
(34) Phillips, M. L. F.; Harrison, W. T. A.; Stucky, G. D.; McCarron, E. M. III; Calabrese, J. C.; Gier, T. E. *Chem. Mater.* **1992**, *4*, 222.
(35) Kunz M.; Brown, I. D. *J. Solid State Chem.* **1995**, *115*, 395.
(36) Munowitz, M.; Jarman, R. H.; Harrison, J. F. *Chem. Mater.* **1993**, *5*, 661.